Supporting Information for

Self-supported Nanoporous $NiCo_2O_4$ Nanowires with Cobalt-nickel Layered Oxide Nanosheets for Overall Water Splitting

Jie Yin,[a] Panpan Zhou,[a] Li An,[a] Liang Huang,[a] Changwei Shao,[c] Jun Wang,[c] Hongyan Liu[a] and Pinxian Xi*[a,b]

[a]Key Laboratory of Nonferrous Metal Chemistry and Resources Utilization of Gansu Province, State Key Laboratory of Applied Organic Chemistry and The Research Center of Biomedical Nanotechnology, Lanzhou University, Lanzhou, 730000, P. R. China.
E-mail: xipx@lzu.edu.cn
[b]Key Laboratory of Advanced Energy Materials Chemistry (Ministry of Education), Nankai University, Tianjin, 300071, P. R. China.
[c]Advanced Ceramic Fibers and Composites laboratory, College of Aerospace Science and Engineering, National University of Defense Technology, Changsha, 410073, P. R. China

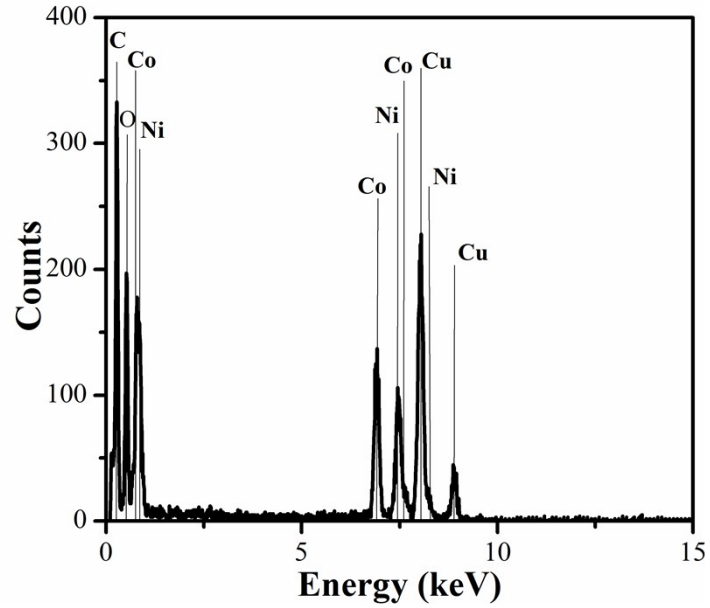

Fig. S1 EDX spectrum for CFP/$NiCo_2O_4$/$Co_{0.57}Ni_{0.43}$LMOs.

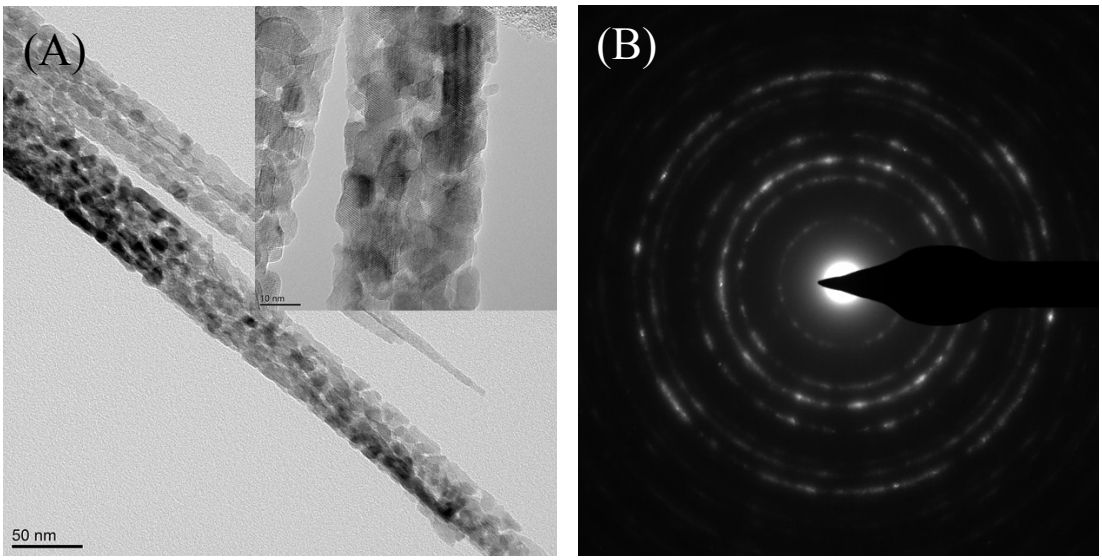

Fig. S2 HR-TEM and SEAD pattern of the $NiCo_2O_4$ NWs.

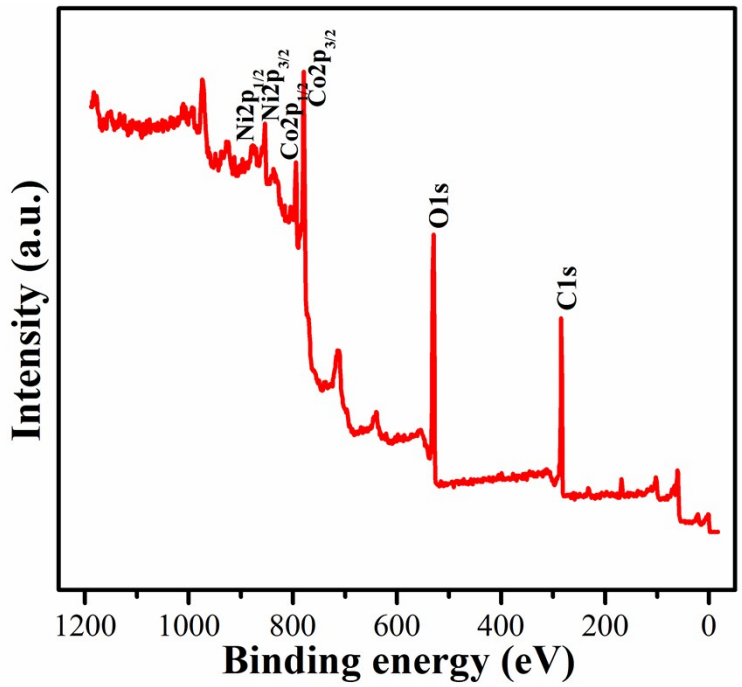

Fig. S3 XPS spectrum for CFP/$NiCo_2O_4$/$Co_{0.57}Ni_{0.43}$LMOs.

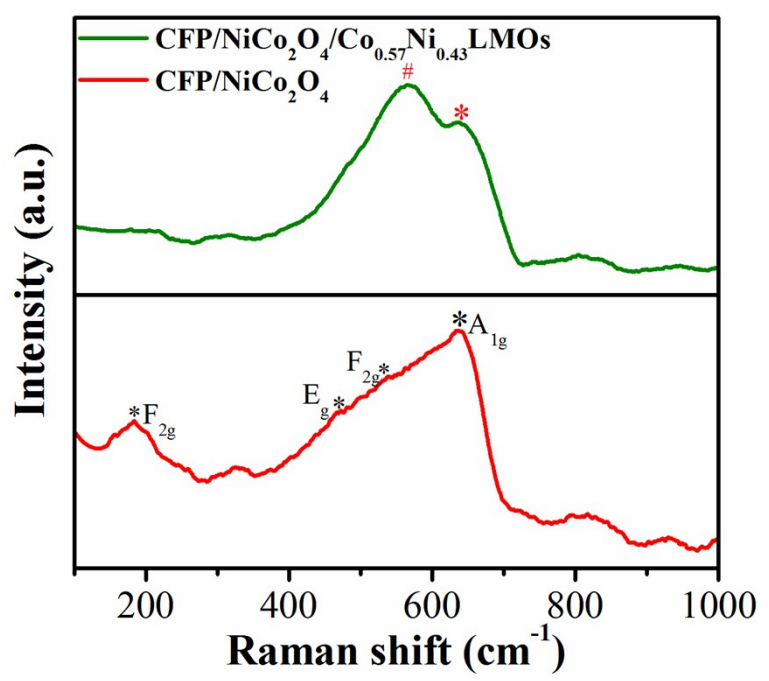

Fig. S4 The Raman spectrem of the CFP/$NiCo_2O_4$ and CFP/$NiCo_2O_4$/$Co_{0.57}Ni_{0.43}$LMOs.

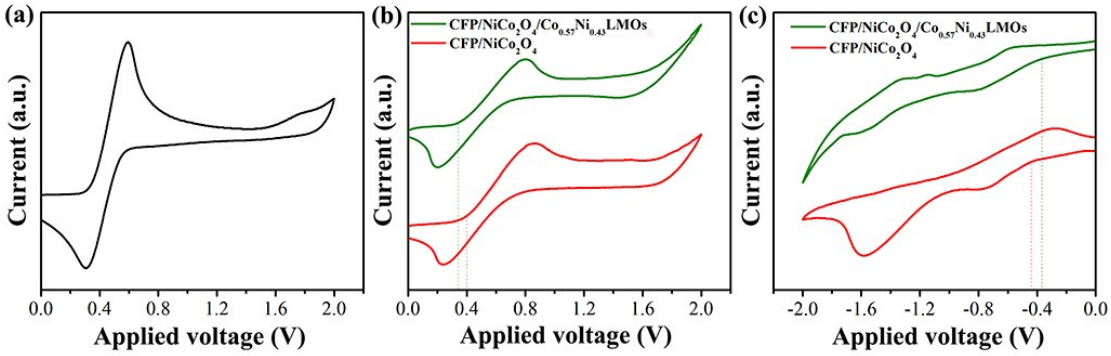

Fig. S5 (a) The cyclic voltammograms (CV) of the oxidation potential of ferrocene as the internal standard to calibrate the measurements, and (b) oxide and (c) reduction CV of CFP/$NiCo_2O_4$ and CFP/$NiCo_2O_4$/$Co_{0.57}Ni_{0.43}$LMOs.

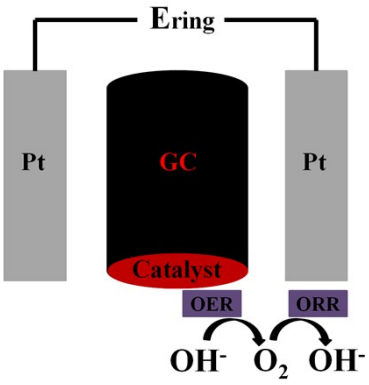

Fig. S6 Schematic illustration of the continous OER (disk electrode) to ORR (ring electrode) process initiated on a RRDE.

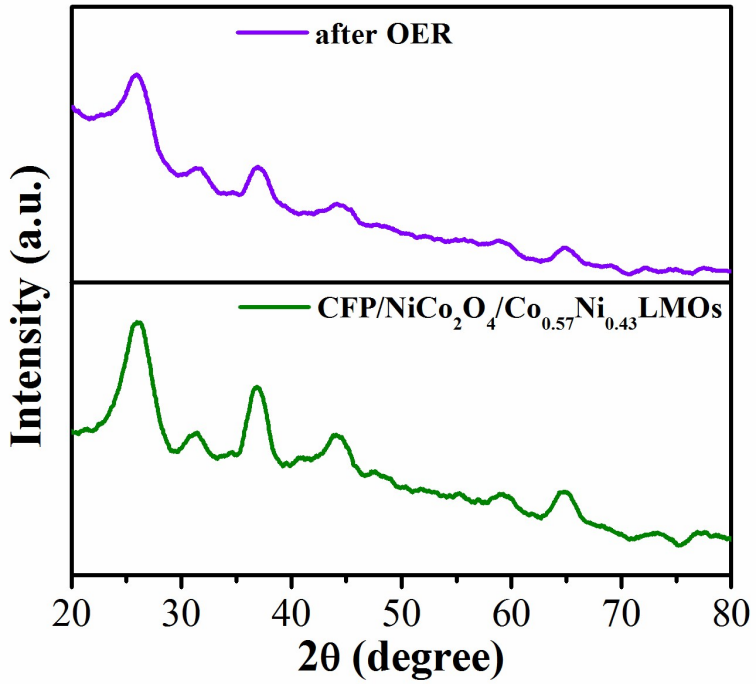

Fig. S7 XRD spectra of CFP/$NiCo_2O_4$/$Co_{0.57}Ni_{0.43}$LMOs before and after the OER stability measurements.

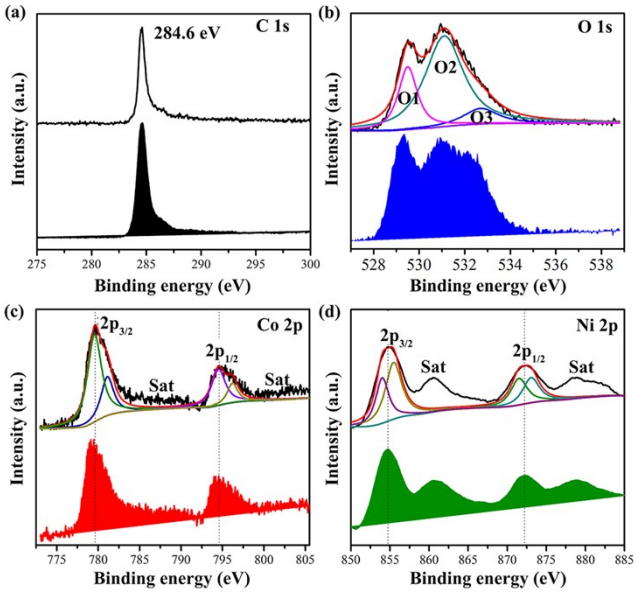

Fig. S8 XPS spectra of (a) C 1s, (b) Co 2p, (c) Ni 2p and (d) O 1s of CFP/$NiCo_2O_4$/$Co_{0.57}Ni_{0.43}$LMOs before and after the OER stability measurements.

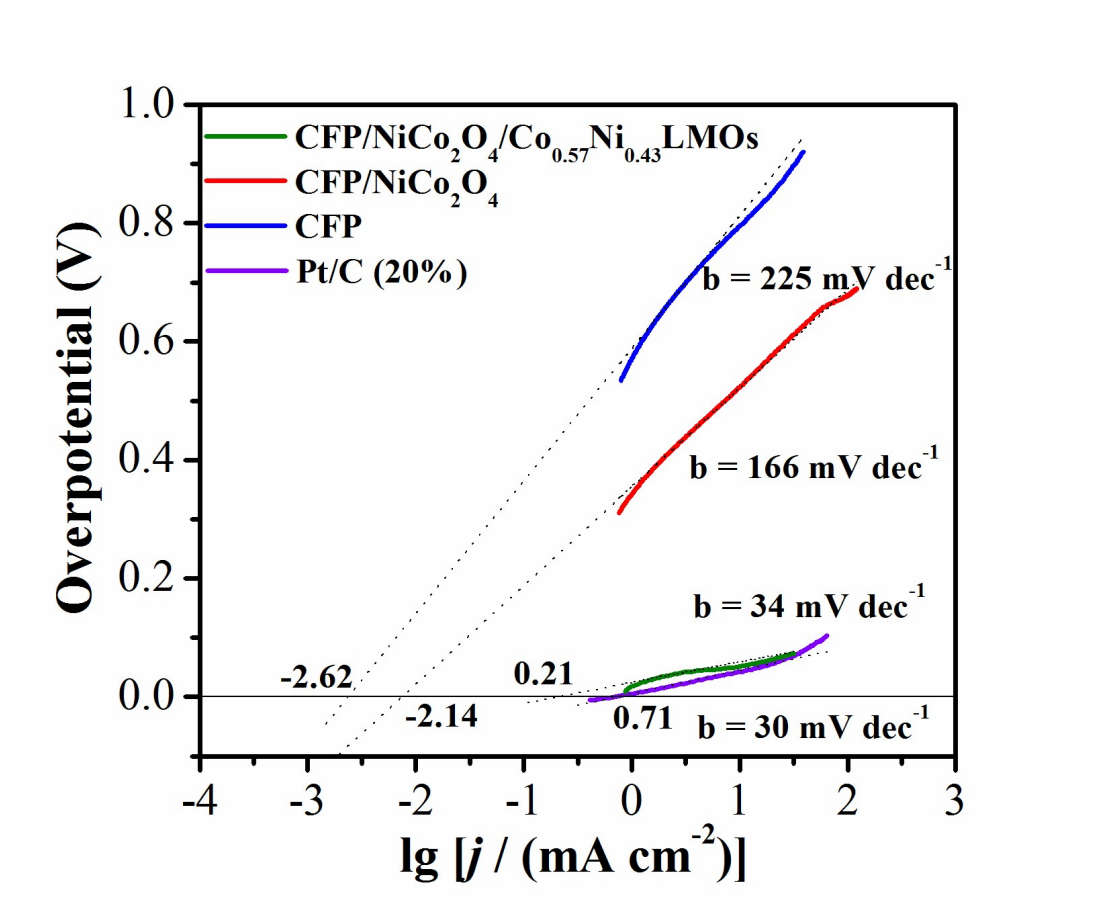

Fig. S9 Calculated exchange current density for CFP, CFP/$NiCo_2O_4$, CFP/$NiCo_2O_4$/$Co_{0.57}Ni_{0.43}$LMOs and Pt/C in 0.5 M H_2SO_4 by applying extrapolation method to the Tafel plot.

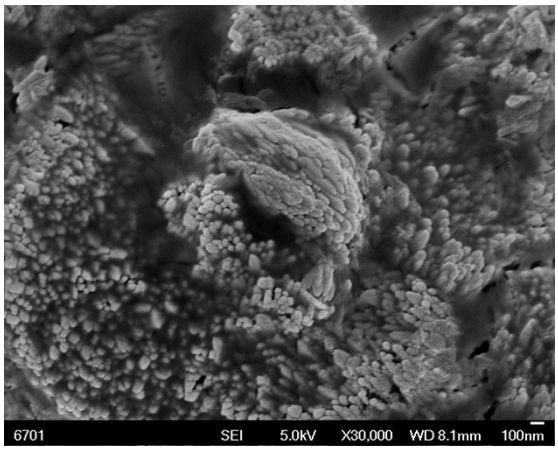

Fig. S10 SEM image of CFP/$NiCo_2O_4$/$Co_{0.57}Ni_{0.43}$LMOs before and after the HER stability measurements.

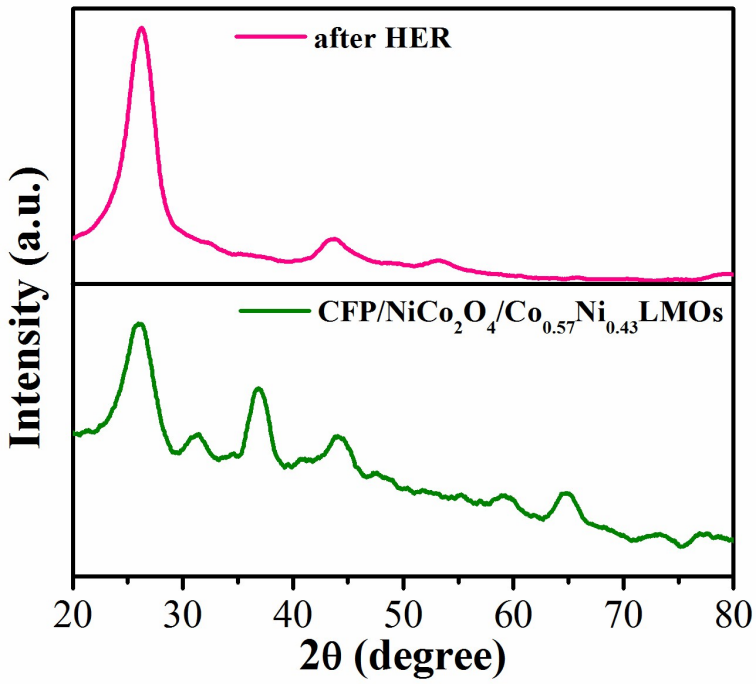

Fig. S11 XRD spectra of CFP/$NiCo_2O_4$/$Co_{0.57}Ni_{0.43}$LMOs before and after the HER stability measurements.

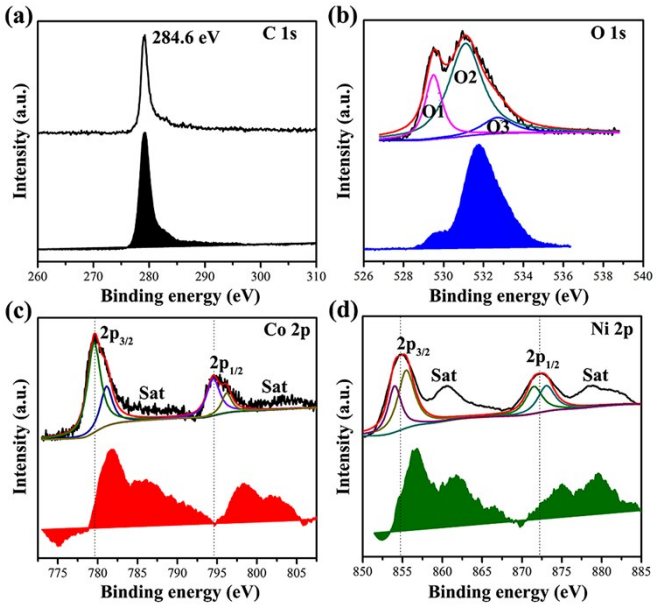

Fig. S12 XPS spectra of (a) C 1s, (b) Co 2p, (d) Ni 2p and (d) O 1s of CFP/$NiCo_2O_4$/$Co_{0.57}Ni_{0.43}$LMOs before and after the HER stability measurements.

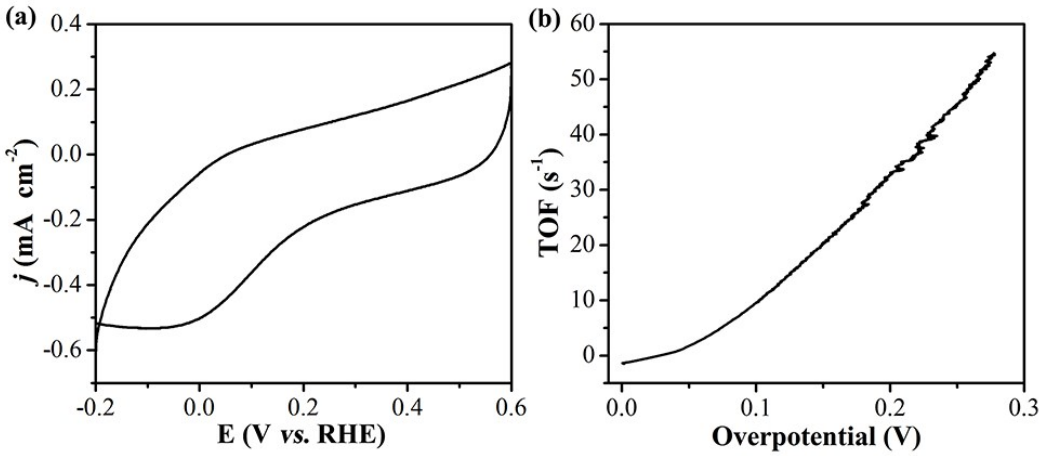

Fig. S13 (a) CV of the CFP/$NiCo_2O_4$/$Co_{0.57}Ni_{0.43}$LMOs in pH = 7 phosphate buffer between -0.2 V and 0.6 V (*vs*. RHE) with a scan rate of 50 mV s^{-1}. (b) Turnover frequencies of the CFP/$NiCo_2O_4$/$Co_{0.57}Ni_{0.43}$LMOs catalyst in 0.5 M H_2SO_4.

Table S1. Comparison of OER performance in alkaline media of CFP/$NiCo_2O_4$/ $Co_{0.57}Ni_{0.43}$LMOs with other OER electrocatalysts

Catalyst	Tafel slope (mV dec^{-1})	Current density (j_0 , mA cm^{-2})	η at the corresponding j (mV)	Ref.
$NiCo_2O_4$	32	285	0.8 (V *vs*. Ag/AgCl)	*Angew. Chem. Int. Ed*., 2015, **54**, 1-7
Co_3O_4	70	10	1.5 (V *vs*. RHE)	*J. Am. Chem. Soc*., 2014, **136**, 13925-13931
$Zn_xCo_{3-x}O_4$	51	10	320	*Chem. Mater*., 2014, **26**, *1889-1895*
NiCo-LDH	40	10	367	*Nano Lett*., 2015, **15**, 1421-1427
$NiCo_2O_4$	63.1	10	320	*Nanoenergy*, 2014, **11**, 021 333-340
$NiCo_2O_4$/FTO	292	5	165	*J. Phys. Chem. C*, 2014, **118**, 25939-25946
		10	323	
NiFe-LDH	30	10	235	*ACS Appl. Mater. Interfaces*, 2014, **6**, 7918-7925
α-$Ni(OH)_2$	42	10	331	*J. Am. Chem. Soc*., 2014, **136**, 7077-7084
Ni−Fe nanoparticles	40	10	280	*Langmuir*, 2014, **30**, 7893-7901
NG-$CoSe_2$	40	10	366	*ACS Nano*., 2014, **8**, 3970-3978
$Mn_xCo_{3-x}O_{4-\delta}$	85	10	1.58 (V *vs*. RHE)	*Chem. Eur. J*., 2014, **20**, 1 - 9
CFP/$NiCo_2O_4$/ $Co_{0.53}Ni_{0.47}$LMOs	63	10	340	In this work
		20	380	

Table S2 OER Electrochemical Parameters of CFP, CFP/$NiCo_2O_4$ and CFP/$NiCo_2O_4$/$Co_{0.57}Ni_{0.43}$LMOs.

Catalyst	R_s (Ohm)	R_{ct} (Ohm)
CFP	14.6	330.4
CFP/$NiCo_2O_4$	19.4	13.5
CFP/$NiCo_2O_4$/$Co_{0.57}Ni_{0.43}$LMOs	15.7	5.2

Table S3. Comparison of HER performance in acid media of CFP/$NiCo_2O_4$/ $Co_{0.57}Ni_{0.43}$LMOs with other HER electrocatalysts

Catalyst	Tafel slope (mV dec^{-1})	Current density (j_0 , mA cm^{-2})	η at the corresponding j (mV)	Ref.
WP_2	57	10	161	*ACS Catal*., 2015, **5**, 145-149
NiP_2 NS/CC	51	10	75	*Nanoscale*, 2014, **6**, 13440-13445
		100	204	
MoP	45	10	90	*Adv. Mater*., 2014, **26**, 5702-5707
		20	105	
MoO_3-MoS_2/FTO	50-60	10	310	*Nano Lett*.**,** 2011, **11**,4168-4175
CoP/CNT	54	2	70	*Angew. Chem. Int. Ed*., 2014, **53**, 6710 –6714
		10	122	
$NiMnN_x$/C	35.9	2	170	*Angew. Chem. Int. Ed*.**,** 2012, **51**, 6131-6135
Ni_2P hollow nanoparticles	46	10	116	*J. Am. Chem. Soc*.**,** 2013, **135**, 9267-9270
		100	180	
CoP hollow nanoparticles	50	20	85	*Angew. Chem. Int. Ed*.**,** 2014, **53**,5427-5430
bulk Mo_2C	56	1	150	*Angew. Chem. Int. Ed*., 2012, **51**, 12703-12706
defect-rich MoS_2	50	13	200	*Adv. Mater*.**,** 2013, **25**, 5807-5813
Co-NRCNTs	69	1	140	*Angew. Chem. Int. Ed*., 2014, **53**, 4372-4376
CFP/$NiCo_2O_4$/ $Co_{0.57}Ni_{0.43}$LMOs	34	10	52	In this work
		100	65.5	

Table S4 HER Electrochemical Parameters of CFP, CFP/$NiCo_2O_4$ and CFP/$NiCo_2O_4$/$Co_{0.57}Ni_{0.43}$LMOs.

Catalyst	R_s (Ohm)	R_{ct} (Ohm)
CFP	2.7	532.9
CFP/$NiCo_2O_4$	2.7	189.3
CFP/$NiCo_2O_4$//$Co_{0.57}Ni_{0.43}$LMOs	1.5	4.5